Fully relativistic calculations of and fits to 1s ionization cross sections

Christopher J. Fontes,[1] Douglas H. Sampson,[2] and Hong Lin Zhang[1]

[1]*Applied Theoretical and Computational Physics Division, Los Alamos National Laboratory, Los Alamos, New Mexico 87545*
[2]*Department of Astronomy and Astrophysics, The Pennsylvania State University, University Park, Pennsylvania 16802*

The range of conditions for which inclusion of the generalized Breit interaction is important in calculating the scattering matrix elements for 1s ionization is explored within the relativistic distorted-wave approximation. This approach is applied to the calculation of 1s ionization cross sections for a variety of ions with one to four bound electrons and nuclear charge Z in the range of $10 \leq Z \leq 92$. These data are then interpolated with simple, but accurate, fit formulas. The resulting expressions are readily integrated over a relativistic Maxwellian electron distribution function to obtain rate coefficients for plasma modeling. A discussion of the high energy behavior of the cross sections for large Z is also given. [S1050-2947(99)08802-2]

PACS number(s): 34.80.Kw

I. INTRODUCTION

In previous work [1] we used the relativistic distorted wave code of [2,3] to calculate cross sections for electron-impact ionization from the $n = 3$, 4, and 5 subshells of various ions. That study included an examination of the cross sections over a range of values for the number of initial bound electrons N and nuclear charge Z. It was found that the reduced cross section [see Eq. (2.8) below] depended only slightly on N and Z in these cases. Hence, the reduced cross sections could be fit with a simple formula that depended solely on impact energy and a simple prescription could be given for obtaining the ionization cross sections for ions of arbitrary complexity. This procedure is especially useful because direct calculation of ionization cross sections for individual cases requires a great deal of computational effort, much more than atomic structure calculations or even collisional excitation calculations.

In the present work we consider ionization from the 1s subshell. This situation is considerably more complex than ionization from the $n = 3$, 4, and 5 subshells for several reasons. First of all the reduced cross sections for 1s ionization vary strongly as a function of Z, as seen from Table II of [2]. This behavior is due to relativistic effects on the tightly bound 1s orbital, which are not important for the $n = 3$, 4, and 5 cross sections. The situation is further complicated by including the generalized Breit interaction (GBI) between bound and free electrons when Z is large. This increases the computational run time by more than two orders of magnitude, but is necessary for accurate results. The GBI increases the 1s ionization cross section by about 50% for $Z = 92$, as was found by electron beam ion trap (EBIT) experiments [4] and by theoretical calculations [5,6], all of which are in excellent agreement. A final consideration is the apparent disagreement of the high Z, high energy behavior between the calculated cross sections and the traditional Bethe high energy formula. Despite these obstacles, as will be shown, we are able to make quite simple, but accurate, Z-dependent fits to the reduced cross sections.

A summary of the purposes of the present work is as follows: (1) to explore the range of conditions for which inclusion of the GBI has a significant effect on cross sections for 1s ionization; (2) to calculate these cross sections (with inclusion of the GBI when significant) for a wide range of energies and for a large number of ions with Z in the range of $10 \leq Z \leq 92$; (3) to explain the high energy behavior of the cross sections for large Z; and (4) to make simple, accurate fits to the corresponding reduced cross sections. These fits should be readily integrated over a relativistic Maxwellian electron distribution function to obtain rate coefficients for plasma applications.

In the next section a description is given of the method for obtaining the cross sections and the procedure for making fits. This is followed by a discussion of the high energy behavior of the cross sections. Finally, the procedure for obtaining rate coefficients is described. Numerical results are given and discussed in Sec. III and the work is summarized in Sec. IV.

II. THEORY

A. Method of calculation

In the present work the atomic structure calculations are made with the Dirac-Fock-Slater (DFS) program of [7], but modified to include the GBI together with other QED corrections plus a distributed nuclear charge, as described in [8]. In the ionization calculations the same potential is used for all electrons bound and free. Hence, all orbitals are automatically orthogonal. For hydrogenic ions this potential is the Coulomb potential $-Z/r$. For complex ions (i.e., those with two or more electrons) we used the DFS potential given by, for example, Eqs. (14)–(16) of [2]. In determining this potential we generally use a mean configuration in which the occupation of the active electron is split between the initial and final subshells. For ionization, this final subshell, which corresponds to that of the ejected electron, is mocked up by a highly excited bound orbital. In the present case this was chosen to be a high lying $\ell = h$ orbital, but results are insensitive to the precise highly excited bound orbital used. Hence, for example, the mean configuration used in the DFS potential for determining the orbitals in the case of inner-shell ionization of Li-like ions initially in the ground level was

$$1s^{1.5}2s9h^{0.5}. \tag{2.1}$$

The GBI is the lowest order quantum electrodynamic correction to the Coulomb interaction. The total interaction, Coulomb plus generalized Breit, is given by

$$g(1,2) = \frac{1}{r_{12}} - (\boldsymbol{\alpha}_1 \cdot \boldsymbol{\alpha}_2)\frac{\exp(i\omega r_{12})}{r_{12}} + (\boldsymbol{\alpha}_1 \cdot \boldsymbol{\nabla}_1)$$

$$\times (\boldsymbol{\alpha}_2 \cdot \boldsymbol{\nabla}_2)\frac{\exp(i\omega r_{12}) - 1}{\omega^2 r_{12}}, \tag{2.2}$$

where $\boldsymbol{\alpha}_1$ and $\boldsymbol{\alpha}_2$ are the usual Dirac matrices and ω is the wave number of the exchanged virtual photon. The importance of inclusion of the GBI was explored for the case of electron-impact excitation in [9,10]. As discussed in [6] and in more detail in [2,3], in order to obtain an ionization computer code from this relativistic distorted wave excitation code one replaces the orbital representing the final excited electron with that representing the ejected electron when calculating the scattering matrix elements. Care must be taken to sum over the appropriate quantum numbers that arise from this orbital replacement, perform the necessary energy integration associated with the presence of two free electrons in the final state, and divide by a factor of π to account for the different normalization between bound and free electrons.

B. Form chosen for the fits to the cross sections

It was shown in [3] that the cross section for ionization of ions of any complexity could be expressed in the form

$$Q(U - U'') = \sum_{\substack{S,S'' \\ S_1,S_1''}} B(U,SS_1;U'',S''S_1'')Q_H^{ps}(n\ell j), \tag{2.3}$$

where S and S_1 are pure states contributing to initial level U, while S'' and S_1'' are pure states contributing to final level U'' with one less bound electron. The B coefficients depend only on the ion properties such as mixing coefficients and angular momenta and are rapidly computed. They are given by Eqs. (36)–(38) of [3], where Eq. (38) of [3] can be easily extended to more complex cases via Eq. (19) of [11]. The pseudohydrogenic cross section $Q_H^{ps}(n\ell j)$ in Eq. (2.3) has exactly the same form as the cross section for electron-impact ionization from subshell $n\ell j$ in a hydrogenic ion except that for nonhydrogenic ions it is calculated using bound and free orbitals determined using the appropriate DFS potential of the actual ion in place of the $-Z/r$ potential.

For the relatively simple cases of principal interest for $1s$ ionization Eq. (2.3) reduces to the simple form

$$Q(U - U'') = BQ_H^{ps}(1s), \tag{2.4}$$

where B has the values

$$B = 1 \tag{2.5}$$

for hydrogenic ions,

$$B = 2 \tag{2.6}$$

for He-like ions and inner-shell ionization of Be-like ions initially in their ground levels, and

$$B = 1/2 \text{ or } 3/2 \tag{2.7}$$

for inner-shell ionization of Li-like ions initially in the ground level when the angular momentum of the final ion is 0 or 1, respectively.

It is convenient to express results in terms of the reduced cross section $Q_R(n\ell j,u)$ defined by

$$Q_H^{ps}(n\ell j) = \frac{\pi a_0^2}{I(\text{Ry})^2} Q_R(n\ell j,u), \tag{2.8}$$

where $I(\text{Ry})$ is the ionization energy in rydbergs and u is the impact electron energy in threshold units

$$u = \epsilon/I. \tag{2.9}$$

A single fit formula for $Q_R(n\ell j,u)$ is fairly accurate for nearly all values of Z and N as long as relativistic effects are not important (see, for example, the results in [1,2]). However, for $1s$ ionization the GBI plus other relativistic effects cause $Q_R(1s,u)$ to increase quite rapidly with Z. This is especially true when u is large. Nevertheless we are able to make quite simple and accurate fits to $Q_R(1s,u)$ using the following procedure.

We take $Z = 20$ as the approximate value above which relativistic effects become significant for the reduced cross sections and first focus our attention on ions for which $Z \geq 20$. We return to the case of $Z < 20$, for which our traditional methods prove quite accurate, near the end of this subsection. As shown by test cases presented in Sec. III the $Q_R(1s,u)$ for a given Z have almost the same values, independent of the number of bound electrons N when $Z \geq 20$. Therefore we need not be concerned with N dependence and choose to fit the hydrogenic $N = 1$ results in this regime. Our strategy is to define a new quantity that will be independent of Z for low impact energies (*u* near 1) and then to fit this quantity to a function of u. To this end we define a new quantity $Q_R'(1s,u)$,

$$Q_R'(1s,u) = Q_R(1s,u)/F(Z), \tag{2.10}$$

where $F(Z)$ is chosen to make $Q_R'(1s,u)$ independent of Z for low impact electron energies. The choice

$$F(Z) = [140 + (Z/20)^{3.2}]/141 \tag{2.11}$$

accomplishes this independence to within 1%. Then for $Z = 20$, where $Q_R' = Q_R$, we fit the calculated results to the form

$$Q_R'(1s,u) = \frac{1}{u}\left\{ A\ln(u) + D\left(1 - \frac{1}{u}\right)^2 + Cu\left(1 - \frac{1}{u}\right)^4 \right. $$

$$\left. + \left[\frac{c}{u} + \frac{d}{u^2}\right]\left(1 - \frac{1}{u}\right)\right\}, \tag{2.12}$$

where $A = 1.13$ is the known constant that reproduces the nonrelativistic Bethe high energy limit and D, C, c, and d are free fit parameters. Except for the term proportional to C, Eq. (2.12) has the same form as the expression used in [1] and earlier work cited therein.

For $Z > 20$ we first tried using Eq. (2.12) with the coefficients A, D, c, and d fixed at the same values as for $Z = 20$ and made best fits to obtain the C parameter at each test Z value. This led to fits that were accurate to within 2.4%. We then used these best values of C to express C as a function of Z. The results, which preserve the accuracy to within 2.4%, are

$$C(Z) = [(Z-20)/50.5]^{1.11} + C(Z=20), \quad 20 \leqslant Z \leqslant 66 \tag{2.13}$$

and

$$C(Z) = [(Z-20)/53]^{0.73} + C(Z=20), \quad 67 \leqslant Z \leqslant 92. \tag{2.14}$$

Moreover, the simple formula

$$C(Z) = [(Z-20)/55]^{0.92} + C(Z=20), \quad 20 \leqslant Z \leqslant 92 \tag{2.15}$$

gives only slightly worse accuracy over the entire range of Z.

Although the $Z = 20$ fit parameters obtained from the above procedure also give a fairly good representation for $Q_R(1s,u)$ for $Z < 20$, further numerical study shows that fitting the He-like, $Z = 10$ results to Eq. (2.12) gives an improved overall accuracy for the low Z region. There is no need to define a quantity like Q'_R for $Z < 20$, or to express C as a function of Z, because there is essentially no Z dependence exhibited by the reduced cross sections in this region.

C. High energy behavior for large Z

The new C term that was added to Eq. (2.12) helps to represent better the rapid increase in the reduced cross section with increasing Z value. However, a second reason for introducing this term is to account for the near-constant behavior exhibited by cross sections at large energies for a fixed value of Z. A graphical example of this behavior is provided in Fig. 1 to complement the explanation that follows. The figure contains hydrogenic results that were calculated with only the Coulomb interaction (''Coulomb only'' curves) and with the Coulomb plus Breit interaction (''Coulomb + Breit'' curves).

Normally one expects the ionization cross section to fall off as $\ln u/u$ (the Bethe formula) at high energies, which is represented by the term proportional to A in Eq. (2.12). However, Bethe's original formula was written in terms of velocities, an expression that holds for relativistic energies. A more appropriate form of the Bethe formula is given by $\ln(\beta^2 + G)/\beta^2$, where β has the usual definition $\beta = v/c$ and G is a constant. This last expression approaches a constant value for very high energies due to the fact that the velocity v of the impact electron is bounded by the speed of light. And, in fact, that is precisely the behavior exhibited by the Coulomb only results in Fig. 1.

In addition, there is a predicted ''relativistic rise'' in the cross section that occurs at sufficiently high impact energies.
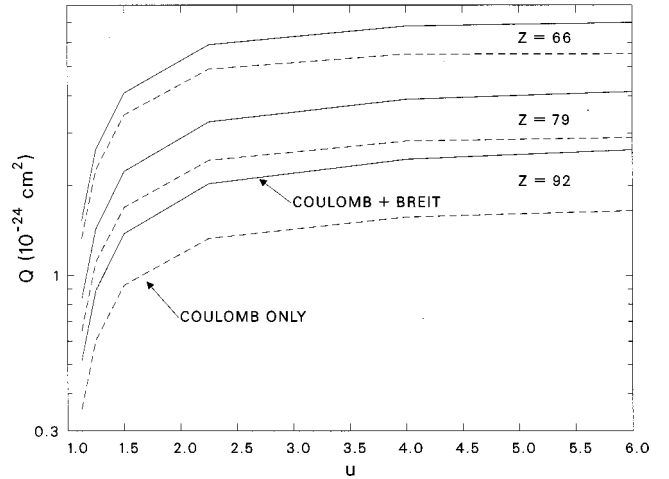

FIG. 1. Ionization cross sections for the $1s$ electron in hydrogenic ions as a function of impact energy in threshold units. Results are given for $Z = 66$, 79, and 92. The dashed lines represent results calculated with only the Coulomb interaction included in the scattering matrix elements. The solid lines represent results calculated with both the Coulomb and Breit interactions.

This rise results when the exchange of a virtual photon, the process represented by the Breit interaction, becomes important (see, for example, the discussion in [12]). The end result of considering a virtual photon exchange is the addition of extra terms to the Bethe formula that grow with increasing impact energy. In particular, the high energy behavior of the cross section is predicted to have the form [12] $\{\ln[\beta^2/(1-\beta^2)] - \beta^2 + G\}/\beta^2$. One can see from the data in Fig. 1 and Table I that the results which include the Breit interaction are increasing slightly faster than the Coulomb only data as the energy and Z value increase. This behavior is an indication that the cross sections are approaching the region in which the relativistic rise occurs. Due to the numerical difficulties associated with obtaining converged cross sections for energies beyond $u = 6$, the highest energy for which detailed cross sections were calculated, we were not able to further explore this behavior. In any event we do not expect our fits to be reliable for u appreciably greater than 6, which is sufficiently large for most practical applications.

D. Formulas for rate coefficients

For high Z ions the temperatures at which $1s$ ionization may become important in a plasma could be sufficiently large as to require a relativistic treatment of the free electron energy distribution. Therefore we assume a relativistic Maxwellian distribution function in determining rate coefficient formulas. With this assumption the rate coefficient for ionization by electron impact is given by

$$\alpha(U - U''; T) = \frac{1}{N_e} \int_{p_0}^{\infty} n_e(p) v Q(U - U'') dp$$

$$= \frac{8\pi e^{-\mu}}{N_e h^3} \int_{p_0}^{\infty} e^{-\epsilon(p)/kT} p^2 v Q(U - U'') dp, \tag{2.16}$$

where N_e is the electron density, p_0 is the momentum corresponding to the threshold of the transition

$$\epsilon(p_0)=I \qquad (2.17)$$

and e^μ is determined by imposing the usual density normalization on the Maxwellian so that

$$e^\mu=\frac{8\pi}{N_e h^3}\int_0^\infty e^{-\epsilon(p)/kT}p^2 dp. \qquad (2.18)$$

Making the change of variables

$$y\equiv\frac{E}{mc^2}, \qquad (2.19)$$

where E is the total energy $\epsilon(p)+mc^2$, we can rewrite Eq. (2.18) as

$$e^\mu=\frac{8\pi(mc)^3 e^{mc^2/kT}}{N_e h^3}\int_1^\infty e^{-(mc^2/kT)y}(y^2-1)^{1/2}y\,dy. \qquad (2.20)$$

With the use of the expressions given in the appendix of [13] this can be expressed as

$$e^\mu=\frac{8\pi}{N_e}\left(\frac{mc}{h}\right)^3\frac{e^a}{a}K_2(a), \qquad (2.21)$$

where $a\equiv mc^2/kT$ and $K_2(a)$ is the modified Bessel function of order 2. For $a>1$ one can expand $K_2(a)$ using Eq. (9.72) of [14] and substitute the results in Eq. (2.21) to obtain

$$e^\mu=\frac{2}{N_e h^3}(2\pi mkT)^{3/2}\left[1+\frac{15}{8}\frac{kT}{mc^2}\right.$$
$$\left.+\frac{105}{108}\left(\frac{kT}{mc^2}\right)^2-\frac{315}{1024}\left(\frac{kT}{mc^2}\right)^3+\cdots\right] \qquad (2.22)$$

in agreement with Eqs. (35) and (36) of [15]. It is easily shown (see, for example, [15]) that

$$v\,dp=d\epsilon \qquad (2.23)$$

relativistically, as well as nonrelativistically. Also

$$p^2=\frac{\epsilon(\mathrm{Ry})}{(a_0/\hbar)^2}\left[1+\frac{\alpha^2}{4}\epsilon(\mathrm{Ry})\right], \qquad (2.24)$$

where α is the fine structure constant. Now we apply Eqs. (2.23) and (2.24) together with Eqs. (2.4), (2.8) and (2.9) to Eq. (2.16) and obtain for the rate coefficient for $1s$ ionization

$$\alpha(1s;T)=\frac{2Be^{-\mu}}{N_e h}\int_1^\infty e^{-(I/kT)u}Q_R(1s,u)u$$
$$\times\left[1+\frac{\alpha^2}{4}I(\mathrm{Ry})u\right]du, \qquad (2.25)$$

where B has the simple values given by Eqs. (2.5)–(2.7) for the cases of interest here. Using Eqs. (2.10)–(2.12) one can perform the integration over energy and obtain

$$\alpha(1s;T)=\frac{2BF(Z)e^{-\mu}}{N_e hb}\left[\left\{\left[(D-3C)+\frac{C}{b}\right]e^{-b}+[A+b(c-2D+6C)]E_1(b)\right.\right.$$

$$+b(D-4C+d-c)E_2(b)+b(C-d)E_3(b)\Big\}$$

$$+\frac{\alpha^2}{4}I(\mathrm{Ry})\left\{\left[(c-D+3C)+\frac{1}{b}(A+D-2C)+\frac{2C}{b^2}\right]e^{-b}\right.$$

$$\left.\left.+\left[b(D+d-c-4C)+\frac{A}{b}\right]E_1(b)+b(C-d)E_2(b)\right\}\right], \qquad (2.26)$$

where it is nearly always valid to use Eq. (2.22) in evaluating $e^{-\mu}$. In Eq. (2.26)

$$b=\frac{I}{kT} \qquad (2.27)$$

and $E_n(b)$ is the nth exponential integral defined by

$$E_n(b)=\int_1^\infty\frac{e^{-bu}}{u^n}du, \qquad (2.28)$$

with properties described in [14]. $F(Z)$ is 1 for $Z\leq 20$ and is given by Eq. (2.11) for higher Z. Also for $Z>20$ the quantity $C=C(Z)$ is given by Eqs. (2.13) and (2.14), or alternatively by Eq. (2.15). Although Eq. (2.26) looks quite lengthy it is very rapidly calculated on a computer. Also for $Z\leq 26$ the part proportional to α^2 will usually be negligible.

III. NUMERICAL RESULTS AND DISCUSSION

First an exploration was made of the range of Z for which inclusion of the GBI is important in calculating the scattering

TABLE I. Comparison of results for $1s$ ionization of hydrogenic ions. The cross sections below are given in units of 10^{-24} cm^2 for various impact electron energies u and nuclear charge Z. Upper entries are values calculated with only the Coulomb interaction included, while lower entries are values calculated with the generalized Breit interaction also included.

				Z				
u	10	20	30	42	50	66	79	92
1.125	2490	155.7	30.8	8.04	4.01	1.327	0.649	0.355
			31.2	8.33	4.27	1.535	0.831	0.516
1.250	4219	264.0	52.3	13.65	6.82	2.259	1.106	0.605
			53.1	14.21	7.29	2.636	1.432	0.889
1.500	6374	399.3	79.2	20.74	10.37	3.453	1.695	0.926
			80.6	21.71	11.19	4.081	2.227	1.381
2.250	8624	542.5	108.3	28.67	14.46	4.897	2.429	1.331
			110.9	30.32	15.82	5.910	3.268	2.029
4.000	8453	538.9	109.9	30.03	15.51	5.503	2.815	1.569
			113.1	32.16	17.28	6.823	3.894	2.450
6.000	7266	471.2	98.6	27.96	14.83	5.512	2.903	1.647
			102.0	30.31	16.80	7.009	4.126	2.639

matrix elements for $1s$ ionization. The results for cross sections calculated for hydrogenic ions with Z values of 10, 20, 30, 42, 50, 66, 79, and 92 and a range of impact energies u in threshold units are given in Table I. The upper entries are

values obtained with only the Coulomb interaction included. The lower entries are those obtained with inclusion of the full interaction given by Eq. (2.2) except that the imaginary part was omitted. Test calculations indicate that the maximum effect of including the imaginary contribution is to increase the cross sections by only 1.6% for energies near threshold when $Z=92$. Hence, the effect is essentially negligible and its omission saves roughly a factor of 2 in computing time. One sees that inclusion of the Breit interaction is very important for high Z, especially for high energies, but the effect steadily decreases with Z and ranges from only 1.3% to 3.4% when $Z=30$. For $Z=10$ and 20 the effect is negligible and hence omitted.

In Table II results for ions in the ground state with various values of N and Z are given in terms of reduced cross sections Q_R, obtained using Eqs. (2.4)–(2.8). Also the ionization energies I(Ry) are listed. For H-like and He-like ions this is the level-level energy, but for Li-like and Be-like ions it is the $1s$ orbital binding energy. Exceptions to this prescription occur at $Z=10$ for which we also give results for the level-level energy in the cases that the final level is listed. One sees that even for $Z=10$, for which the effect of electron correlation should be greatest, there is hardly any difference between the Q_R values determined with these various energies for a given N value. Hence, for higher Z the Q_R for Li-like and Be-like ions were determined using only the orbital binding energy for I(Ry).

TABLE II. Reduced cross sections $Q_R(1s,u)$ and ionization energies I(Ry) for ions in the ground state with various N and Z values. Here $y[n]$ means $y\times10^n$.

Z	N	Final Level	I(Ry)	$u=\epsilon/I$ 1.125	1.250	1.500	2.250	4.000	6.000
10	1		1.0013[2]	0.2837	0.4807	0.7264	0.9828	0.9632	0.8280
	2		8.7797[1]	0.2714	0.4580	0.7038	0.9682	0.9669	0.8396
	3		8.4376[1]	0.2636	0.4557	0.6951	0.9694	0.9768	0.8495
	3	$(1s2s)_0$	8.4793[1]	0.2647	0.4577	0.6982	0.9744	0.9819	0.8539
	3	$(1s2s)_1$	8.4007[1]	0.2626	0.4539	0.6923	0.9650	0.9721	0.8455
	4		8.0893[1]	0.2587	0.4434	0.6824	0.9600	0.9790	0.8574
	4	$(1s2s^2)_{1/2}$	8.0795[1]	0.2584	0.4430	0.6816	0.9588	0.9777	0.8563
20	1		4.0205[2]	0.2861	0.4851	0.7337	0.9968	0.9901	0.8657
	2		3.7688[2]	0.2793	0.4743	0.7217	0.9882	0.9896	0.8682
	3		3.6975[2]	0.2774	0.4722	0.7196	0.9886	0.9942	0.8733
	4		3.6213[2]	0.2730	0.4679	0.7142	0.9862	0.9960	0.8766
23	1		5.3261[2]	0.2873	0.4871	0.7369	1.0030	1.0017	0.8822
30	1		9.1063[2]	0.2943	0.5003	0.7602	1.0450	1.0659	0.9610
42	1		1.8062[3]	0.3091	0.5269	0.8051	1.1244	1.1927	1.1240
50	1		2.5869[3]	0.3245	0.5545	0.8509	1.2030	1.3143	1.2779
	2		2.5181[3]	0.3198	0.5469	0.8407	1.1904	1.3012	1.2642
	3		2.5036[3]	0.3192	0.5461	0.8400	1.1907	1.3027	1.2655
	4		2.4825[3]	0.3173	0.5432	0.8361	1.1869	1.2995	1.2623
66	1		4.6373[3]	0.3751	0.6444	0.9976	1.4447	1.6678	1.7134
	2		4.5389[3]	0.3702	0.6352	0.9850	1.4270	1.6468	1.6905
79	1		6.8591[3]	0.4446	0.7660	1.1912	1.7477	2.0825	2.2067
	2		6.7311[3]	0.4383	0.7554	1.1754	1.7248	2.0546	2.1764
92	1		9.7078[3]	0.5531	0.9522	1.4798	2.1740	2.6247	2.8273
	2		9.5422[3]	0.5455	0.9391	1.4599	2.1451	2.5903	2.7942
	3		9.5407[3]	0.5459	0.9394	1.4614	2.1481	2.5950	2.8024
	4		9.4934[3]	0.5431	0.9394	1.4545	2.1389	2.5845	2.7890

TABLE III. Calculated values (upper entries) for $Q_R'(1s,u) = Q_R(1s,u)/F(Z)$, where $F(Z)$ is given by Eq. (2.10). Lower entries are fits of $Q_R'(1s,u)$ to Eq. (2.12) with $C=C(Z)$ given by Eqs. (2.13) and (2.14).

			$u=\epsilon/I$			
Z	1.125	1.250	1.500	2.250	4.000	6.000
20	0.2861	0.4851	0.7337	0.9968	0.9901	0.8657
	0.2865	0.4843	0.7333	0.9993	0.9875	0.8666
23	0.2862	0.4852	0.7340	0.9990	0.9977	0.8787
	0.2865	0.4843	0.7338	1.0035	1.0013	0.8876
30	0.2889	0.4910	0.7461	1.0257	1.0462	0.9432
	0.2865	0.4845	0.7353	1.0151	1.0399	0.9466
42	0.2891	0.4928	0.7531	1.0517	1.1156	1.0514
	0.2865	0.4849	0.7382	1.0372	1.1133	1.0584
50	0.2882	0.4924	0.7557	1.0684	1.1672	1.1349
	0.2865	0.4851	0.7402	1.0528	1.1650	1.1372
66	0.2849	0.4895	0.7578	1.0974	1.2668	1.3015
	0.2866	0.4857	0.7444	1.0852	1.2728	1.3014
79	0.2835	0.4885	0.7596	1.1145	1.3280	1.4072
	0.2866	0.4860	0.7466	1.1023	1.3297	1.3882
92	0.2866	0.4935	0.7669	1.1266	1.3602	1.4652
	0.2867	0.4863	0.7487	1.1185	1.3832	1.4698

For $Z\geq 20$ one sees from the results in Table II that the dependence on N is weak. More specifically, a maximum difference of 4.8% occurs near threshold between the $N=1$ and 4 values for $Z=20$. The differences in the reduced cross sections for different N values at higher energies and Z values are progressively smaller. Hence, the results for H-like ions with $Z=20$ have been chosen in determining the fit parameters for this regime. If the reader desires extremely high accuracy in the cross sections for a number of bound electrons other than one, a different set of fit parameters can always be generated from the relevant values in Table II using the procedure described in Sec. II B. However, our results generated from the hydrogenic cross sections should be accurate enough (within about 5%) for most purposes.

Values of $Q_R'(1s,u)$, which is obtained from Q_R via Eqs. (2.10) and (2.11), are listed in Table III. Upper entries are the calculated values of Q_R' and the lower entries are the fits to Q_R' obtained as described in Sec. II B. One sees that Q_R' at energies close to threshold is nearly independent of Z. The fit parameters obtained from fitting the hydrogenic results for $Q_R'=Q_R$ when $Z=20$ are listed in Table IV. For $Z>20$ these same fit parameters are used to calculate Q_R' via Eq. (2.12) except that C is replaced with $C(Z)$ given by Eqs. (2.13) and (2.14). The maximum errors in the fits listed in Table III are 2.4% and 2.0%, occurring at $u=1.5$ for $Z=92$ and 50, respectively. If instead $C(Z)$ given by Eq. (2.15) is used, the maximum error is 2.5%, which occurs at $u=6$ for $Z=30$.

For $Z<20$ one sees that the Q_R in Table II exhibit the strongest N dependence, as expected. To help mitigate this dependence we chose to fit the results for He-like ions with $Z=10$, rather than the hydrogenic results, as the best compromise in the low Z regime. The fit parameters obtained by

TABLE IV. Parameters for fits to Q_R by use of Eq. (2.12) for hydrogenic ions with $Z=20$ and heliumlike ions with $Z=10$.

Z	N	A	D	c	d	C
10	2	1.1300	3.82652	-0.80414	2.32431	0.14424
20	1	1.1300	3.70590	-0.28394	1.95270	0.20594

applying Eq. (2.12) to the $Z=10$, $N=2$ values for Q_R given in Table II are also displayed in Table IV.

In summary, both sets of fit parameters listed in Table IV are to be used in Eq. (2.26) for rates, or Eqs. (2.4), (2.8), and (2.10)–(2.12) for cross sections. The $Z=20$ parameters are also to be used for ions with $Z>20$, provided the above prescription for properly choosing the C coefficient is followed. More specifically, the C coefficient should be determined from Eqs. (2.13) and (2.14), or from Eq. (2.15). For $Z<20$ both sets of parameters do a good job of fitting the cross sections because the Q_R are reasonably insensitive to changes in Z in this region. From Table II we find a maximum difference of 5.9% between the calculated Q_R values for $Z=10$, $N=2$ and $Z=20$, $N=1$. Since each set of parameters reproduces the calculated Q_R values from which they were determined to within 0.4%, we conclude that either set will give good results for $Z<20$. However, to obtain the best possible fits we recommend using the $Z=20$, $N=1$ values for $16\leq Z<20$ and the $Z=10$, $N=2$ values for $Z\leq 15$. This choice should give moderately accurate results down to atoms that have lost three or more electrons.

IV. SUMMARY

A fully relativistic distorted wave method has been used to explore the range of conditions for which inclusion of the GBI has a significant effect on cross sections for ionization from the $1s$ subshell. A discussion of the resulting high energy behavior of the cross sections for large Z has also been given. Results are expressed conveniently in terms of reduced cross sections Q_R. Based on the calculated values for a large number of ions with $10\leq Z\leq 92$, quite simple fits have been made that allow one to readily calculate $1s$ ionization cross sections and rate coefficients for ions with one to four bound electrons. These fits are valid for a large range of systems, from low Z atoms a few times ionized up to those with $Z=92$. For most of this range the results are expected to be quite accurate, within about 5%, but the accuracy will progressively lessen as one considers low Z, near-neutral species.

In future work it is planned to consider ionization from the $n=2$ subshell, where the Breit interaction is also expected to be important for high Z, but somewhat less so than for $1s$ ionization.

[1] C. J. Fontes, D. H. Sampson, and H. L. Zhang, Phys. Rev. A **48**, 1975 (1993).

[2] H. L. Zhang and D. H. Sampson, Phys. Rev. A **42**, 5378 (1990).

[3] D. H. Sampson and H. L. Zhang, Phys. Rev. A **45**, 1657 (1992).

[4] R. E. Marrs, S. R. Elliot, and D. A. Knapp, Phys. Rev. Lett. **72**, 4082 (1994).

[5] D. L. Moores and K. J. Reed, Phys. Rev. A **51**, R10 (1995).

[6] C. J. Fontes, D. H. Sampson, and H. L. Zhang, Phys. Rev. A **51**, R12 (1995).

[7] D. H. Sampson, H. L. Zhang, A. K. Mohanty, and R. E. H. Clark, Phys. Rev. A **40**, 604 (1989).

[8] D. H. Sampson, H. L. Zhang, and C. J. Fontes, At. Data Nucl. Data Tables **48**, 25 (1991).

[9] C. J. Fontes, D. H. Sampson, and H. L. Zhang, Phys. Rev. A **47**, 1009 (1993).

[10] C. J. Fontes, D. H. Sampson, and H. L. Zhang, Phys. Rev. A **49**, 3704 (1994).

[11] H. L. Zhang and D. H. Sampson, Phys. Rev. A **47**, 208 (1993).

[12] U. Fano, Phys. Rev. **102**, 385 (1956).

[13] D. P. Kilcrease and R. C. Kirkpatrick, Nucl. Fusion **28**, 1465 (1988).

[14] *Handbook of Mathematical Functions,* edited by M. Abramowitz and I. A. Stegun (Dover, New York, 1970).

[15] D. H. Sampson and H. L. Zhang, J. Quant. Spectrosc. Radiat. Transf. **54**, 345 (1995).